

Quantitative Analysis of TM Lateral Leakage in Foundry Fabricated Silicon Rib Waveguides

Anthony P. Hope, Thach G. Nguyen, Arnan Mitchell, and Wim Bogaerts

Abstract—We show that thin, shallow ridge, silicon-on-insulator waveguides exhibiting a lateral leakage behavior can be designed and fabricated using a standard silicon photonic foundry platform. We analyze the propagation loss through the observation of the transmitted TM polarized guided mode and TE polarized radiation and experimentally demonstrate that propagation losses as low as 0.087 dB/mm can be achieved. This demonstration will open a new frontier for practical devices exploiting a lateral leakage behavior with potential applications in the fields of biosensing and quantum optics among others.

Index Terms—Silicon-on-insulator, integrated circuit technology, optical waveguides.

I. INTRODUCTION

IT HAS been shown that silicon waveguides with exceptionally low loss can be achieved using a shallow ridge configuration [1]. It was predicted that these waveguides should exhibit strong vertical evanescence when operated in the TM polarization, with potential applications for hybrid integration [2] and biosensing [3]. However, it was found experimentally that the TM mode only achieved low loss transmission for a discrete set of waveguide widths, an effect not predicted by traditional simulators used for initial predictions [4].

This phenomenon has been theoretically explained due to phase matching (Fig. 1(a)) of the fundamental guided TM mode of the ridge and the TE radiation (in the cladding) [4], [5]. The magnitude of this coupling is controlled by interference effects (Figs. 1(b,c)). Certain waveguide widths either coherently cancel the radiation (Figs. 1(d,e)), or completely reinforce it resulting in the strongest losses (Fig. 1(f)).

It follows naturally that this strong polarization dependent radiation can be used to realize compact integrated polarizers [6] or variable attenuators [7], but rather than viewing this effect as a simple loss mechanism, one can consider it as a means of generating controlled coherent beams of TE light [8], with one possible application being long-range transfer of an optical carrier between apparently uncoupled waveguides [9]. The analysis of most of the proposed structures harnessing

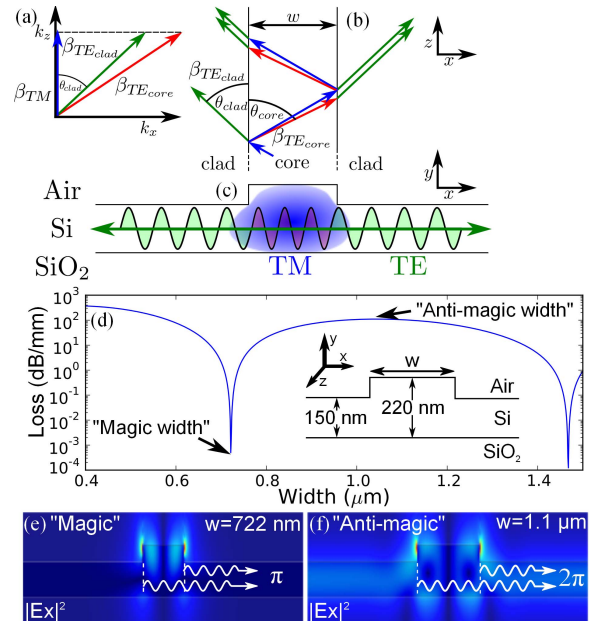


Fig. 1. The fundamental TM mode is altered and *hybridized* in shallow etched waveguides; (a) At certain in-plane angles, the radiative TE modes of the silicon slabs ($\beta_{TE_{core}}$ and $\beta_{TE_{clad}}$) can be phase matched to the fundamental guided TM mode (β_{TM}), (b) interference is responsible for the appearance of ‘magic’ values where the radiation produced by either sidewall is interfering destructively, and this effect is related to the width (w) of the waveguide and the operational wavelength (λ), (c) a representation of the mode profile of the hybridized TM-like mode containing both vertical and horizontal components, (d) the width dependence of the propagation loss of the fundamental TM mode, (e) at ‘magic width’ ($w = 722$ nm) the lateral radiation cancels out and the waveguide has a low propagation loss. (f) At ‘anti-magic width’ ($w = 1.1$ μm) the radiation is reinforced and results in a strong field presence in the cladding.

lateral leakage has been limited to simulation. Implementing the experimental approach of [1] and [4] requires non-standard processing which may be difficult to access.

In this letter, we show that lateral leakage can be reliably achieved using standard silicon foundry fabrication. We observe the width dependent leakage loss through the transmission of the TM mode and also observe the leaked TE radiation directly. Our observations match well with predictions. This standard fabrication platform offers benefits such as high precision, repeatability, throughput and the possibility of inclusion in multiple project wafer initiatives (MPW), lowering fabrication costs. This demonstration will improve the understanding and confidence in the operation of lateral leakage so that new and interesting devices can be developed and adopted into industrial integrated silicon photonic systems. Preliminary material from this work was published in [10]; however, here we present deeper analysis and substantial additional results.

Manuscript received January 26, 2015; revised August 3, 2015; accepted November 6, 2015. Date of publication November 12, 2015; date of current version January 20, 2016. This work was supported by the Australian Research Council under Grant CE110001018 and Grant DP1096153.

A. P. Hope, T. G. Nguyen, and A. Mitchell are with the ARC Centre of Excellence for Ultrahigh Bandwidth Devices for Optical Systems, School of Electrical and Computer Engineering, RMIT University, Melbourne, VIC 3000, Australia (e-mail: anthony.hope@student.rmit.edu.au; thach.nguyen@rmit.edu.au; arnan.mitchell@rmit.edu.au).

W. Bogaerts is with the Center of Nano- and Biophotonics, Photonics Research Group, Department of Information Technology, Ghent University-imec, Ghent 9000, Belgium, and also with Luceda Photonics, Dendermonde 9200, Belgium (e-mail: wim.bogaerts@ugent.be).

Color versions of one or more of the figures in this letter are available online at <http://ieeexplore.ieee.org>.

Digital Object Identifier 10.1109/LPT.2015.2500233

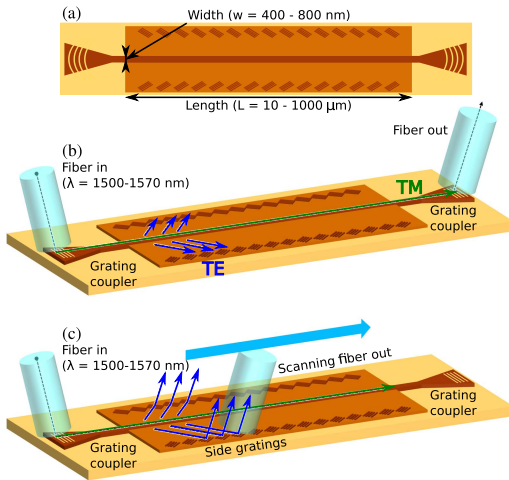


Fig. 2. (a) Schematic of the fiber measurement procedure for multiple defined waveguides with varying widths ($w = 400\text{--}800\text{ nm}$) and lengths ($L = 10\text{--}1000\ \mu\text{m}$), (b) measuring the transmission of TM light through the waveguides, (c) collecting the converted TE light received at the side gratings with a scanning fiber or imaged with an infrared camera.

II. DESIGN OF THIN SHALLOW RIDGES FOR CMOS FABRICATION AND GRATING COUPLER CHARACTERISATION

This section aims to show that thin shallow ridge waveguides exhibiting lateral leakage can be realized using standard silicon photonic fabrication. We chose the ePIXfab IMEC standard platform using 220 nm thick silicon on 2 μm silicon dioxide, patterned with either 70 nm or full 220 nm etching with minimum features sizes of 150 and 130 nm, respectively [11]. The upper cladding was air. The devices were designed and simulated using the ‘IPKISS’ framework [12] and a custom eigenmode expansion model [13] to enable simulation of the lateral leakage behaviour. Our simulations predicted that ridges with these parameters, should support a single TM mode at a wavelength of 1550 nm up to a width of about 850 nm. Fig. 1(d) presents the predicted lateral leakage loss as a function of ridge width, clearly showing low-loss ‘magic’ width behaviour at a width of 722 nm.

We designed a series of waveguides with a range of widths from 400–800 nm and lengths 10 μm –1 mm. Each waveguide was interfaced to single mode fibers using tapered focussed TM grating couplers [14], [15] designed for optimum efficiency in the $\lambda = 1500\text{--}1570\text{ nm}$ range and phase matched only to the TM mode. To observe the TE lateral leakage radiation, a series of grating couplers, phase matched and oriented to align with the expected TE radiation, were included on either side of the waveguide along its length. The very different phase velocities of the TE and TM slab modes ensures only the TE mode is out-coupled by this grating. Fig. 2(a) presents a schematic of the designed structure and Figs. 2(b-c) illustrate the methods for measuring the TM waveguide transmission and the TE lateral leakage radiation, respectively.

The designed devices were fabricated, and to determine the actual waveguide dimensions, a sample of devices were cross-sectioned and imaged using scanning electron microscopy (SEM). An SEM image of one of the realized structures is presented in Fig. 3. The silicon thickness was found to be 215 nm, the ridge was 70 nm and the ridge widths tended to be 10–20 nm wider than the nominal design.

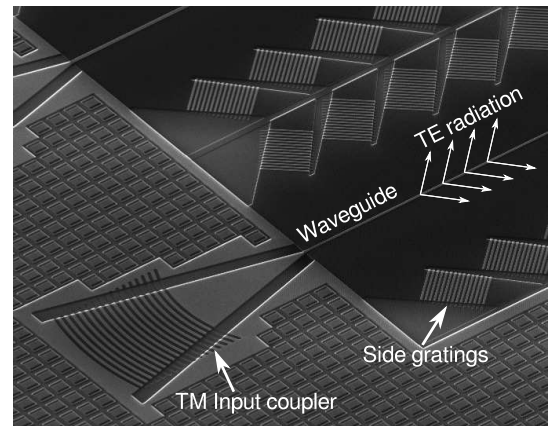


Fig. 3. Scanning electron microscope image of the input section of our fabricated waveguides, showing the input focussed TM coupler, waveguide and side TE gratings. All outer regions have been completely etched to isolate each individual waveguide from another.

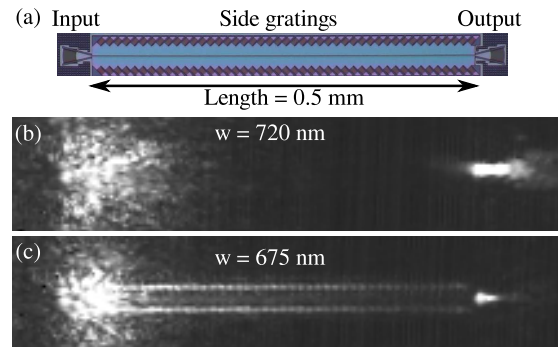


Fig. 4. (a) Optical microscope image of a fabricated waveguide of length 0.5 mm, including input, output and side grating couplers, (b) infrared imaging of a 720 nm wide waveguide which is close to the predicted ‘magic’ low loss condition, (c) infrared imaging of a 675 nm wide ‘non-magic’ waveguide demonstrates how light is converted to TE radiation away from this resonance.

Simulating with the slab thickness at 215 nm, we found that the predicted ‘magic’ width is 717 nm at a wavelength of 1550 nm. From this point, all reported dimensions are as-fabricated.

To qualitatively test the structures, an infrared camera was positioned above the 0.5 mm long waveguides and the input coupler was excited with a wavelength of 1550 nm. Fig. 4(a) shows a visible wavelength microscope image of one of the waveguide structures. Fig. 4(b) shows the infrared image of the 720 nm wide waveguide excited at 1550 nm. On the input side we see scattered light. On the output side we see a very bright spot corresponding to light exiting through the output TM grating coupler. In between we see darkness indicating that light is confined within the waveguide.

Fig. 4(c) shows an infrared camera image of the 675 nm wide waveguide excited at 1550 nm. Again we see scattered light from the input. The light at the output TM grating coupler is dimmer than in Fig. 4(c). In between we see excitation of the TE side gratings, decreasing with distance from the input. Fig. 4(c) presents clear evidence of lateral leakage behaviour in thin-ridge waveguides while Fig. 4(b) presents clear evidence of the suppression of lateral leakage when the waveguide is ‘magic’ width. Together these represent the first evidence of lateral leakage observed in mass fabricated silicon waveguides.

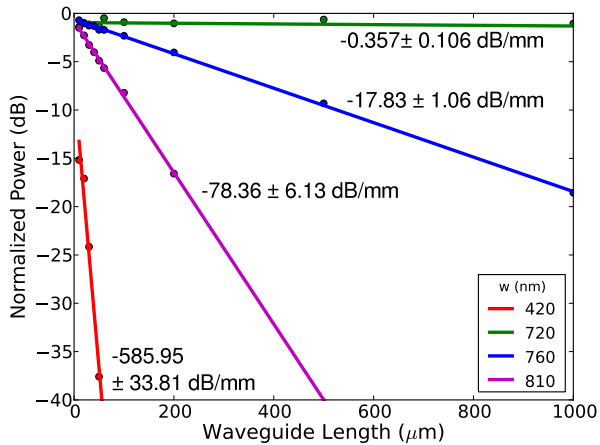


Fig. 5. TM transmission at $\lambda = 1550$ nm vs waveguide length for different waveguide widths. The gradient yields the waveguide propagation loss (α).

III. WAVEGUIDE CHARACTERIZATION

A. Width Dependent Propagation Loss

We first quantify the propagation loss as a function of waveguide width using the cut-back method, measuring the transmission efficiency for identical waveguides of different lengths and then extract the loss per unit length. The transmission of waveguides of widths 420, 720, 760 and 820 nm and lengths between 10 and 1000 μm were each measured at a wavelength of 1550 nm and the transmission efficiency as a function of length is plotted in Fig. 5. To eliminate the response of the grating couplers, a fully etched wire waveguide of width 420 nm with identical grating couplers was used as a normalization reference. The propagation loss (α) is the slope of the line in dB/mm. These results clearly show that there is a strong dependence of observed loss on waveguide width with $\alpha = 0.357$ dB/mm when $w=720$ nm rising to $\alpha = 585.95$ dB/mm, similar to the behaviour reported in [4].

B. Wavelength Dependent Propagation Loss

Lateral leakage is a resonant effect and thus we expect the loss to not only depend on ridge width, but also on wavelength [4]. For 1550 nm, we expect ‘magic’ width behaviour, where the lateral leakage loss is completely cancelled, at a width of 717 nm. To characterize the wavelength dependent propagation loss, we measured the power transmitted through waveguides with widths of 675, 700, 720 and 740 nm over the entire fabricated length range, while scanning the wavelength from 1500–1570 nm as illustrated in Fig. 2(b). The loss of each waveguide width was again determined using a linear fit.

Fig. 6 presents the transmitted power per unit length for each waveguide as a function of wavelength. Resonant loss cancellation is clearly evident with waveguide widths of 700 nm and 720 nm exhibiting minimal loss of 0.238 dB/mm and 0.087 dB/mm at wavelengths of 1500 nm and 1563 nm, respectively.

The expected wavelength dependent lateral leakage behaviour was simulated using eigenmode expansion [13] and these predictions are also presented in Fig. 6. An excellent match to the measured values is evident, particularly the 720 nm width waveguide with transmission loss approaching zero at the resonant wavelength.

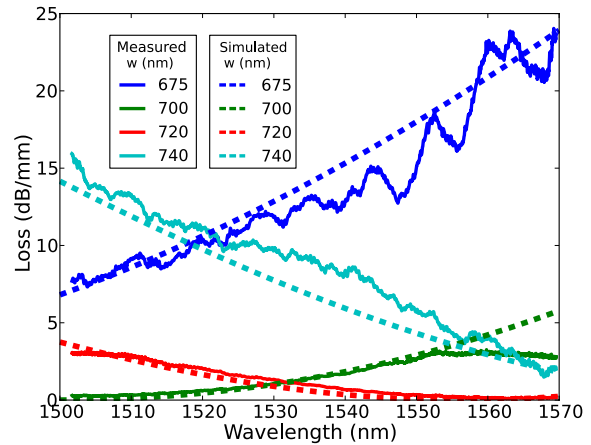


Fig. 6. The wavelength dependant TM transmission loss of four fabricated waveguide widths. Simulations have been performed to compare the spectral response of each waveguide width.

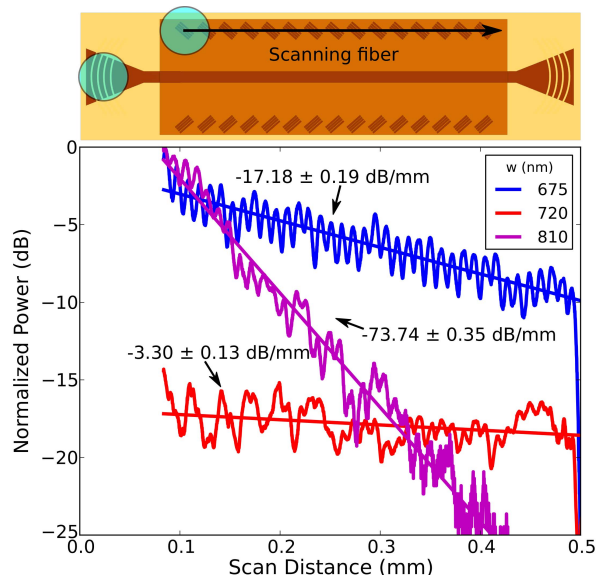


Fig. 7. Scanning an output fiber across the center of these side gratings provides quantitative information regarding the TE conversion and the loss can be estimated with a linear fit.

C. Conversion of TM Guided Propagation to TE Radiation

To observe the TE radiation we use side gratings, with period and orientation for efficient diffraction of the TE mode propagating at the expected angle of 45 degrees, as illustrated in Fig. 2(c). Waveguides of fabricated widths $w = 675, 720$ and 810 nm and length 500 μm were excited with $\lambda = 1550$ nm and the intensity measured at the TE side gratings as a function of length is presented in Fig. 7. The rapid oscillations are due to the numerous, discrete side gratings. A linear fit to each trace indicates exponential decay with the slope yielding the the attenuation coefficient. These are similar to those of Fig. 6 indicating that the observed width dependent loss is due to conversion of the TM guided light into lateral TE radiation.

IV. ANALYSIS OF LEAKAGE MEASUREMENTS

We have characterized the fabricated thin ridge waveguides over a wide range of wavelengths, widths and lengths,

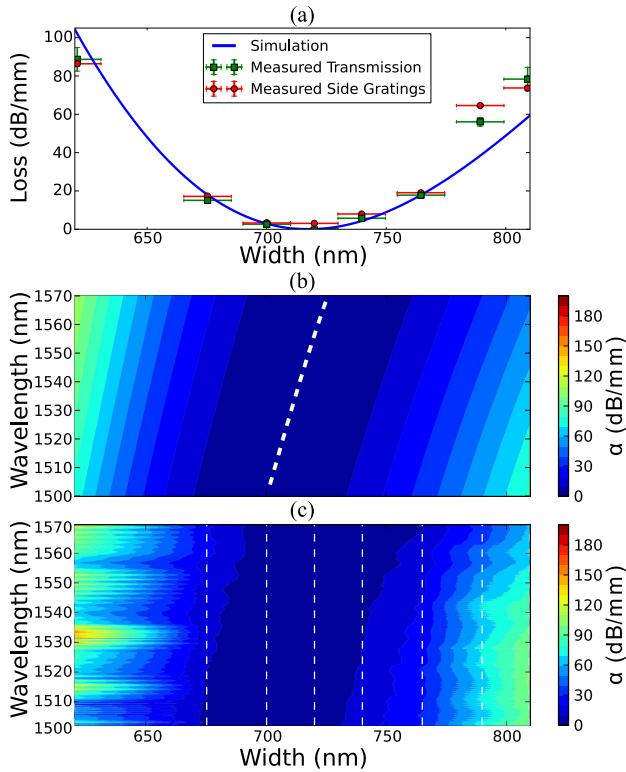


Fig. 8. (a) Experimental propagation loss obtained from the transmission measurements and side grating measurements, compared to the simulated loss at $\lambda = 1550$ nm. (b) Simulation of the propagation loss (α) expected for 215 nm high, 70 nm etched air clad SOI waveguides as a function of waveguide width and wavelength, the ideal magic width is dashed white. (c) Propagation loss (α) calculated from the interpolated experimental transmission data, which is in good agreement with the simulation.

and we have compared these measurements with simulations based on the measured as-fabricated waveguide parameters. Cut-back analysis of the direct TM transmission loss (Fig. 5) and the observation of the TE radiation (Fig. 7) was used to extract the propagation loss. Fig. 8(a) presents a survey of the propagation loss as a function of waveguide width at $\lambda = 1550$ nm extracted from both the measured TM transmission and TE radiation. The vertical and horizontal error bars represent uncertainty in the measured loss and dimensional accuracy (± 10 nm), respectively. The predicted loss of the fundamental waveguide mode due solely to TE radiation, is also presented in Fig. 8(a). Excellent agreement between both measurements and prediction is evident up to widths of 760 nm. At widths above 780 nm, the waveguide is expected to begin to support a strongly radiating higher order resonance, which becomes a guided mode at 850 nm, and this may explain the additional transmission loss observed at these widths and above.

A wavelength sweep was also conducted during the measurements. Fig. 8(b) and (c) present the predicted and interpolated, experimentally measured propagation loss as a function of waveguide width and λ , respectively. Again we find a very good match, with a slight skew towards the higher waveguide widths.

V. CONCLUSION

We have shown that thin, shallow-etched SOI waveguides exhibiting lateral leakage behaviour can be realized using standard, silicon photonic foundry fabrication. We have characterized the waveguides via analysis of the transmitted TM mode and also direct observation of the TE radiation. We find very good correspondence between eigenmode expansion predictions and two different measurement procedures. Magic width behaviour with resonant cancellation of the leakage leading to losses as low as 0.087 dB/mm have been observed experimentally. The ability to design, simulate and experimentally realize these passive waveguide structures using a standard silicon photonic fabrication platform creates new opportunities for practical design and accessible fabrication of realizable devices exploiting lateral leakage with potential applications including biophotonic sensing and quantum information processing.

REFERENCES

- [1] R. Pafchek, R. Tummidi, J. Li, M. A. Webster, E. Chen, and T. L. Koch, "Low-loss silicon-on-insulator shallow-ridge TE and TM waveguides formed using thermal oxidation," *Appl. Opt.*, vol. 48, no. 5, pp. 958–963, 2009.
- [2] R. S. Tummidi, R. M. Pafchek, K. Kim, and T. L. Koch, "Modification of spontaneous emission rates in shallow ridge 8.3 nm erbium doped silica slot waveguides," in *Proc. IEEE Group IV Photon. Conf.*, Sep. 2009, pp. 226–228.
- [3] K. Kim, R. M. Pafchek, and T. L. Koch, "Label-free biosensors based on athermal silicon-on-insulator waveguides and a harmonic dithering technique," in *Proc. CLEO Sci. Innov. OSA*, May 2012, pp. 1–2.
- [4] M. A. Webster, R. M. Pafchek, A. Mitchell, and T. L. Koch, "Width dependence of inherent TM-mode lateral leakage loss in silicon-on-insulator ridge waveguides," *IEEE Photon. Technol. Lett.*, vol. 19, no. 6, pp. 429–431, Mar. 15, 2007.
- [5] T. G. Nguyen, R. S. Tummidi, T. L. Koch, and A. Mitchell, "Lateral leakage of TM-like mode in thin-ridge silicon-on-insulator bent waveguides and ring resonators," *Opt. Exp.*, vol. 18, no. 7, pp. 7243–7252, 2010.
- [6] D. Dai, Z. Wang, N. Julian, and J. E. Bowers, "Compact broadband polarizer based on shallowly-etched silicon-on-insulator ridge optical waveguides," *Opt. Exp.*, vol. 18, no. 26, pp. 27404–27415, 2010.
- [7] T. Ako, J. Beekman, W. Bogaerts, and K. Neyts, "Tuning the lateral leakage loss of TM-like modes in shallow-etched waveguides using liquid crystals," *Appl. Opt.*, vol. 53, no. 2, pp. 214–220, 2014.
- [8] N. Dalvand, T. G. Nguyen, T. L. Koch, and A. Mitchell, "Thin shallow-ridge silicon-on-insulator waveguide transitions and tapers," *IEEE Photon. Technol. Lett.*, vol. 25, no. 2, pp. 163–166, Jun. 15, 2013.
- [9] A. P. Hope, T. G. Nguyen, A. D. Greentree, and A. Mitchell, "Long-range coupling of silicon photonic waveguides using lateral leakage and adiabatic passage," *Opt. Exp.*, vol. 21, no. 19, pp. 22705–22716, 2013.
- [10] A. P. Hope, T. G. Nguyen, W. Bogaerts, and A. Mitchell, "Experimental demonstration of TM lateral leakage in a standard SOI photonics platform," in *Proc. Group IV Photon.*, Aug. 2014, pp. 77–78.
- [11] S. K. Selvaraja, P. Jaenen, W. Bogaerts, D. Van Thourhout, P. Dumon, and R. Baets, "Fabrication of photonic wire and crystal circuits in silicon-on-insulator using 193-nm optical lithography," *J. Lightw. Technol.*, vol. 27, no. 18, pp. 4076–4083, Sep. 15, 2009.
- [12] M. Fiers *et al.*, "Improving the design cycle for nanophotonic components," *J. Comput. Sci.*, vol. 4, no. 5, pp. 313–324, Sep. 2013.
- [13] T. G. Nguyen, R. S. Tummidi, T. L. Koch, and A. Mitchell, "Rigorous modeling of lateral leakage loss in SOI thin-ridge waveguides and couplers," *IEEE Photon. Technol. Lett.*, vol. 21, no. 7, pp. 486–488, Apr. 1, 2009.
- [14] F. Van Laere *et al.*, "Compact focusing grating couplers for silicon-on-insulator integrated circuits," *IEEE Photon. Technol. Lett.*, vol. 19, no. 23, pp. 1919–1921, Dec. 1, 2007.
- [15] D. Vermeulen *et al.*, "Efficient tapering to the fundamental quasi-TM mode in asymmetrical waveguides," in *Proc. ECIO*, 2010, pp. 1–2.